Search For Electron-Antineutrinos Associated With Gravitational-Wave Events at Daya Bay

Huiyou Chen, Tsinghua University, China.

On behalf of the Daya Bay collaboration

F. P. An et al 2021 Chinese Phys. C 45 055001

1. Daya Bay Experiment [1]

The Daya Bay Experiment provides precise measurement of reactor anti-neutrino disappearance via Inverse Beta Decays (IBDs), and the IBDs are tagged by neutron capture on gadolinium (nGd) or on hydrogen (nH).

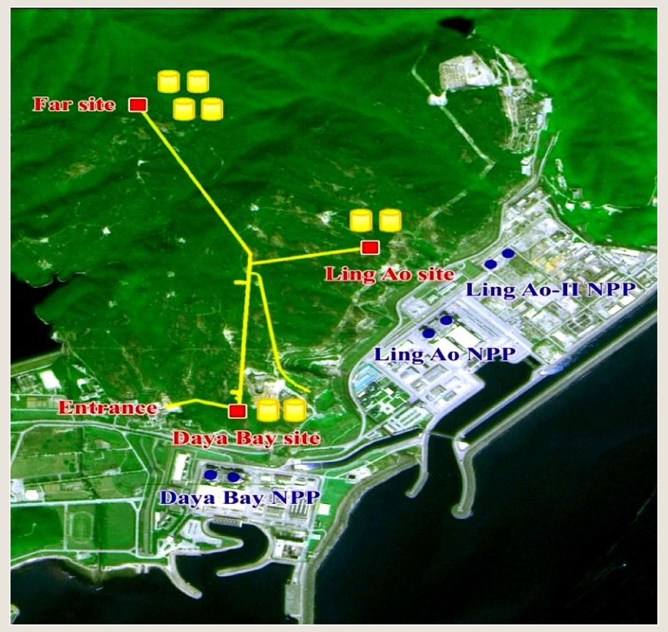

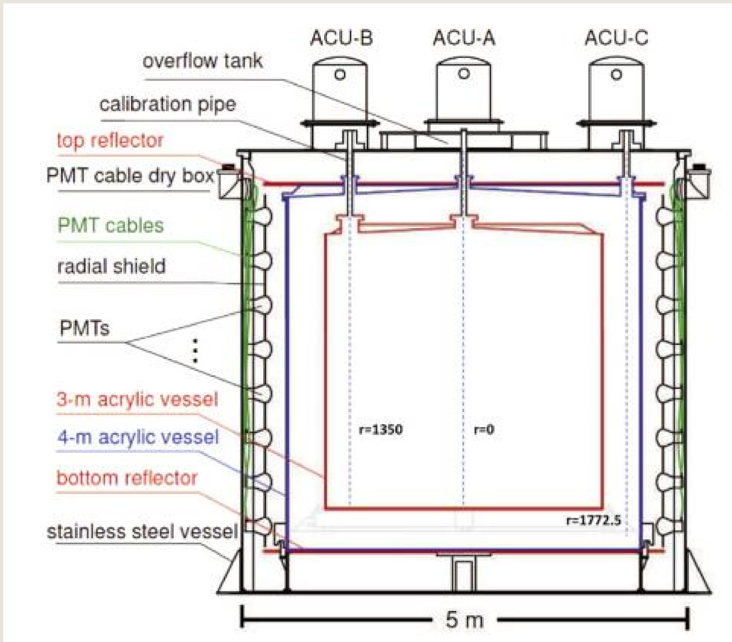

- 6 low enriched uranium (LEU) commercial reactors, each with 2.9 GW thermal power.
- These reactors provide abundant electron-antineutrinos.

2. Gravitational-Wave Events

- The direct observation of gravitational waves (GWs) provides an important probe for investigating the dynamical origin of high-energy cosmic transients.
- Providing a possible connection between neutrino emission and gravitational-wave (GW) bursts is important to our understanding of the physical processes that occur when black holes or neutron stars merge.
- A list of GWs of interest for this study is listed [2-8].

GW events	Type of merged bodies	Detection time (UTC)	Distance D_{LIGO} (Mpc)
GW150914	Black holes	2015.09.14 09:50:45	410^{+160}_{-180}
GW151012	Black holes	2015.10.12 09:54:43	1100^{+500}_{-500}
GW151226	Black holes	2015.12.26 03:38:53	440^{+180}_{-190}
GW170104	Black holes	2017.01.04 10:11:58	880^{+450}_{-390}
GW170608	Black holes	2017.06.08 02:01:16	340^{+140}_{-140}
GW170814	Black holes	2017.08.14 10:30:43	540^{+130}_{-210}
GW170817	Neutron stars	2017.08.17 12:41:04	40^{+8}_{-14}

3. Neutrino Fluence Measurement Method

- We limited our search for $\bar{\nu}_e$ with energies below 100 MeV.
- To accommodate the uncertainties, we adopted three time windows to search for neutrino bursts associated with the GW events, ±10 s, ±500 s , ±1000 s .
- We first measured the electron-antineutrino fluence, Φ_{FD},with a normalized, pinched Fermi-Dirac spectrum, with zero chemical potential and a pinching factor of $\eta = 0$, as applied in the KamLAND experiment [9]. Using the number of electron-antineutrino candidates N_ν within the searching window, the electron-antineutrino fluence is calculated as

$$\Phi_{\mathrm{FD}} = \frac{N_\nu}{N_p \int \sigma(E_\nu)\epsilon(E_\nu)\phi(E_\nu)dE_\nu}, \qquad \phi(E_\nu) = \frac{1}{T^3 F_2(\eta)} \frac{E_\nu^2}{e^{E_\nu/T-\eta}+1},$$

- Where N_p is the number of target protons, $\sigma(E_\nu)$ is the IBD cross-section and $\epsilon(E_\nu)$ is the detector efficiency.
- For the Monochromatic Spectra,

$$\Phi_{\mathrm{D}}(E_\nu) = \frac{N_\nu}{N_p \sigma(E_\nu)\epsilon(E_\nu)}.$$

4. Data Analysis

- IBD candidate selection [10]

	nGd	nH
Basic	AD Trigger and flasher cut	
AD muon	> 100 MeV	
AD muon veto	(0, 800) μs	
Pool muon [IWS, OWS]	$N_{\mathrm{IWS\ PMT}} > 12$ or $N_{\mathrm{OWS\ PMT}} > 15$	
Pool muon veto	(0, 600) μs	
Shower muon	> 2.5 GeV	
Shower muon veto	(0, 1) s	
Coincidence time	(1, 200) μs	(1, 400) μs
Delayed energy	(6, 12) MeV	Peak ± $3\sigma_E$
Coincidence distance	N/A	< 100 cm
Prompt energy (basic)	N/A	> 3.5 MeV
Prompt energy (window)	Signal searching region	

- Prompt-energy spectra of the neutrino candidates

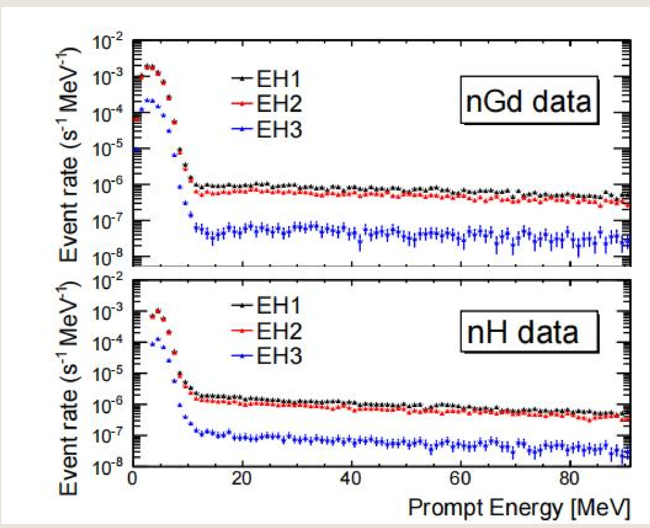

- Background
- In all possible cases, we used the realtime estimation, i.e. the result in ±5 days around a GW, for background estimation. But when the background is very low, we used the average of the entire data set.
- Average background rate (per second per antineutrino detector).

	EH1	EH2	EH3
		nGd	
Low E	$(7.65\pm0.01)\times10^{-3}$	$(6.82\pm0.01)\times10^{-3}$	$(8.45\pm0.01)\times10^{-4}$
High E	$(6.35\pm0.04)\times10^{-5}$	$(4.32\pm0.04)\times10^{-5}$	$(3.83\pm0.08)\times10^{-6}$
		nH	
Low E	$(28.75\pm0.04)\times10^{-4}$	$(25.76\pm0.03)\times10^{-4}$	$(3.25\pm0.01)\times10^{-4}$
High E	$(9.20\pm0.05)\times10^{-5}$	$(6.30\pm0.05)\times10^{-5}$	$(5.65\pm0.10)\times10^{-6}$

- Low E : E < 10MeV.
- High E : E >10MeV.

- Candidates and background comparison(result for GW150914 as an example)

		nGd Low E	nGd High E	nH Low E	nH High E
EH1-AD1	Candidate	4	0	4	0
	BKG. (±5 days)	6.96 ± 0.08	0.060 ± 0.008	2.52 ± 0.06	0.080 ± 0.009
	BKG. (Averaged)	7.65 ± 0.01	0.064 ± 0.001	2.88 ± 0.01	0.092 ± 0.001
EH1-AD2	Candidate	5	0	1	0
	BKG. (±5 days)	6.95 ± 0.08	0.054 ± 0.007	2.54 ± 0.05	0.072 ± 0.008
	BKG. (Averaged)	7.65 ± 0.01	0.064 ± 0.001	2.88 ± 0.01	0.092 ± 0.001
EH2-AD1	Candidate	4	0	2	0
	BKG. (±5 days)	6.62 ± 0.08	0.037 ± 0.006	2.37 ± 0.05	0.041 ± 0.006
	BKG. (Averaged)	6.82 ± 0.01	0.043 ± 0.001	2.58 ± 0.01	0.063 ± 0.001
EH2-AD2	Candidate	8	0	1	0
	BKG. (±5 days)	6.46 ± 0.08	0.027 ± 0.005	2.35 ± 0.05	0.056 ± 0.006
	BKG. (Averaged)	6.82 ± 0.01	0.043 ± 0.001	2.58 ± 0.01	0.063 ± 0.001
EH3-AD1	Candidate	0	0	0	0
	BKG. (±5 days)	0.97 ± 0.03	0.004 ± 0.002	0.37 ± 0.02	0.008 ± 0.003
	BKG. (Averaged)	0.850 ± 0.001	0.0038 ± 0.0001	0.330 ± 0.001	0.0056 ± 0.0001
EH3-AD2	Candidate	0	0	0	0
	BKG. (±5 days)	1.00 ± 0.03	0.003 ± 0.002	0.36 ± 0.02	0.007 ± 0.003
	BKG. (Averaged)	0.850 ± 0.001	0.0038 ± 0.0001	0.330 ± 0.001	0.0056 ± 0.0001
EH3-AD3	Candidate	0	0	0	0
	BKG. (±5 days)	0.97 ± 0.03	0.001 ± 0.001	0.34 ± 0.02	0.004 ± 0.002
	BKG. (Averaged)	0.850 ± 0.001	0.0038 ± 0.0001	0.330 ± 0.001	0.0056 ± 0.0001
EH3-AD4	Candidate	1	0	0	0
	BKG. (±5 days)	0.97 ± 0.03	0.007 ± 0.002	0.36 ± 0.02	0.005 ± 0.002
	BKG. (Averaged)	0.850 ± 0.001	0.0038 ± 0.0001	0.330 ± 0.001	0.0056 ± 0.0001

- In all cases, the number of candidates is consistent with the background number.

- Detection efficiency
- The signal detection efficiency is defined as [10]

$$\epsilon = \epsilon_\mu \cdot \epsilon_m \cdot \epsilon_{other}$$

$$\epsilon_{other} = \sum_v (N_{p,v} \cdot \epsilon_{Ep,v} \cdot \epsilon_{Ed,v} \cdot \epsilon_{D,v} \cdot \epsilon_{T,v}) / \sum_v N_{p,v}.$$

- ϵ_μ : muon veto efficiency.
- ϵ_m : the multiplicity cut efficiency for the two-fold event selection.
- $\epsilon_{Ep,v}, \epsilon_{Ed,v}, \epsilon_{D,v}, \epsilon_{T,v}$ correspond to the prompt energy, delayed energy, coincident distance (for the nH sample only), and coincident-time efficiency, respectively.

5. Upper Limits on $\bar{\nu}_e$ Fluence

- Under two different neutrino spectrum assumptions,upper limits (90% C.L.) of fluence for three search time windows are listed.

Fluence ($\times10^{10}$ cm^{-2})	Monochromatic Spectra								Fermi-Dirac Spectrum
E_ν	5 MeV	7 MeV	10 MeV	20 MeV	30 MeV	50 MeV	70 MeV	90 MeV	(1.8, 100) MeV
±10 s	11.3	4.7	1.6	0.55	0.25	0.10	0.05	0.02	0.70
±500 s	20.6	10.5	1.9	0.53	0.25	0.10	0.05	0.02	0.63
±1000 s	24.4	8.1	1.9	0.55	0.25	0.10	0.05	0.02	0.54

- For the Monochromatic Spectra, we plot the results in the table above below.

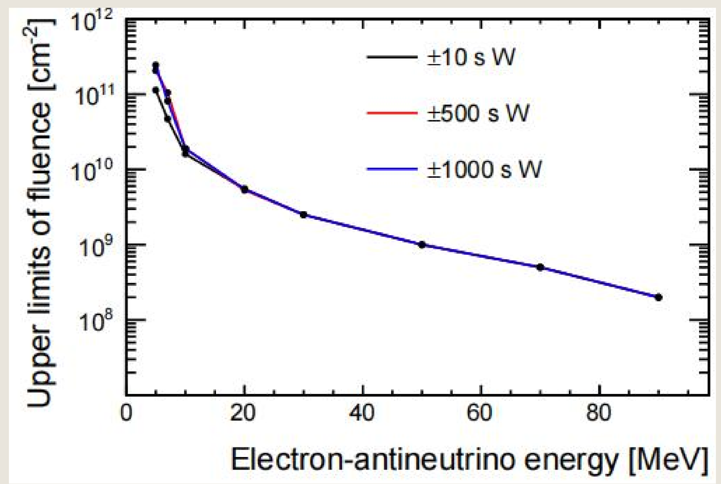

6. References

[1] F.P. An et al, Nucl. Instrum. Meth. A 811, (2016) 133-161
[2] B. Abbott et al. (LIGO Scientific, Virgo), Phys. Rev. Lett. 119, 161101 (2017)
[3] B. Abbott et al. (LIGO Scientific, Virgo), Phys. Rev. Lett. 116, 061102 (2016)
[4] B. Abbott et al. (LIGO Scientific, Virgo), Phys. Rev. D 93, 122003 (2016)
[5] B. P. Abbott et al. (LIGO Scientific, Virgo), Phys. Rev. Lett. 116, 241103 (2016)
[6] B. P. Abbott et al. (LIGO Scientific, VIRGO), Phys. Rev. Lett. 118, 221101 (2017)
[7] B. P. Abbott et al. (LIGO Scientific, Virgo), Astrophys. J. 851, L35 (2017)
[8] B. Abbott et al. (LIGO Scientific, Virgo), Phys. Rev. Lett. 119, 141101 (2017)
[9] A. Gando et al. (KamLAND), Astrophys. J. 829, L34 (2016), [Erratum: Astrophys.J. 851, L22 (2017)]
[10] F. P. An et al. (Daya Bay), Phys. Rev. D 95, 072006 (2017)